Effect of dislocations on open circuit voltage in crystalline silicon solar cells

Thomas Kieliba,[a] Stephan Riepe, and Wilhelm Warta
Fraunhofer Institute for Solar Energy Systems, Heidenhofstrasse 2, 79110 Freiburg, Germany

(Received 29 March 2006; accepted 1 August 2006; published online 8 November 2006)

The dislocation dependence of open circuit voltage is studied based on Donolato's model for the effect of dislocations on minority carrier effective diffusion length [J. Appl. Phys. **84**, 2656 (1998)]. Experimental data measured on thin-film solar cells show a strong decrease of open circuit voltage V_{oc} with an increase in defect density. The analysis of the recombination currents indicates that V_{oc} is largely reduced by space charge region recombination. For a quantitative study on the relationship between dislocation density, effective diffusion length, and V_{oc} the data are fitted with an extended version of Donolato's model. Taking into account the base recombination current as well as the space charge region recombination current, the modeled curves fit very well to the experimental data. However, satisfactory fitting results require that the region of high recombination is set wider than the "effective depletion region width," which is calculated from the electrical field strength in a planar *p-n* junction. This effect can be explained with the assumption of a geometrical enlargement of the *p-n* junction due to defects like dislocations. © *2006 American Institute of Physics*. [DOI: 10.1063/1.2360773]

I. INTRODUCTION

For multicrystalline Si solar cells, short circuit current as well as open circuit voltage depend on dislocation density.[1–3] The short circuit current is affected by dislocations mainly through a reduction of minority carrier lifetime (or diffusion length) in the device's base. Donolato has developed an analytical model describing the effect of dislocations on effective diffusion length.[4] This concept has been used to model experimental data measured on different kinds of Si solar cells and multicrystalline Si wafers.[5–9] Donolato has also used his model to calculate the effect of dislocations on open circuit voltage V_{oc} of an illuminated diode.[10] However, in these calculations only the effect of the base saturation current on V_{oc} was considered. In devices like thin-film solar cells, recombination in the space charge region (SCR) significantly contributes to the saturation current.[11,12] The objective of this work is to develop a quantitative model for the dependence of V_{oc} on dislocation density based on measurements on crystalline Si thin-film solar cells.

II. EXPERIMENT

The investigated thin-film solar cells are composed of a supporting substrate, an insulating intermediate layer, and the active Si thin-film, which consists of a recrystallized *p*+ Si seed film and an epitaxially grown *p* Si layer. This stack represents a silicon on insulator (SOI) structure. Based on a tight control of recrystallization conditions and layer thickness we were able to prepare samples with different, well-defined dislocation densities.

Standard 650 μm thick Czochralski (Cz)-Si wafers served as substrates. They were covered with a 1 μm thick thermally grown insulating oxide. On top of the oxide, a Si film of either 2 or 8 μm thickness was prepared as follows: Firstly, 0.5 μm of undoped Si was deposited by low-pressure chemical vapor deposition (LPCVD). Subsequently, this layer was thickened by either 1.5 or 7.5 μm of highly boron doped (10^{19} cm^{-3}) Si deposited by atmospheric pressure chemical vapor deposition (APCVD). Then the Si film was processed by zone-melting recrystallization (ZMR). In this way, grain size could be enlarged to typically several millimeters in width and several centimeters in length. Among others, defect density of the ZMR films depends on the crystal growth speed, being determined by the scan speed, and the Si film thickness.[3,13–16] Varying the scan speed between 10 and 100 mm mm^{-1}, Si films with different dislocation densities could be prepared reproducibly. During ZMR processing, the Si film was coated with a 150 nm thick thermally grown oxide to prevent agglomeration of the molten Si. After recrystallization, this oxide was removed in HF. The 8 μm thick films were additionally treated with a CP133 etch [solution of HF (50%), CH_3COOH, and HNO_3 in the ratio 1:3:3], removing in average 1.5 μm of the Si film, and revealing the grain structure. The recrystallized film then served as seed for a subsequent epitaxial growth. In this way, a 30 μm thick Si layer with a doping concentration of 8×10^{16} cm^{-3} was grown by APCVD. Again, the finished Si film was treated with a CP133 etch.

From the final Si films, two sets of test thin-film solar cells were processed, with a mesa structure and 1 cm^2 active area. Set 1 was prepared with a simple process without bulk passivation and without antireflection coating (ARC). This set of samples was used to study the effect of seed film thickness and ZMR scan speed for ten different combinations. For selected combinations from the same group of Si

[a]Author to whom correspondence should be addressed; present address: ErSol Solar Energy AG, Wilhelm-Wolff-Strasse 23, 99099 Erfurt, Germany; FAX: +49 361 2195-205; electronic mail: thomas.kieliba@ersol.de

TABLE I. Technological parameters of analyzed samples together with measured values of dislocation density and effective diffusion length. The thicknesses W_1 and W_2, respectively, refer to the final thickness in the solar cell, taking into account reduction by etching steps.

ZMR seed film thickness (μm)	p+layer thickness W_2 (μm)	ZMR scan speed ν (mm/min)	p layer thickness W_1 (μm)	Dislocation density ρ_d (cm^{-2})	Effective diffusion length $L_{\mathrm{eff,IQE}}$ (μm)
8	6.5	20	27	8.9×10^6	30
8	6.5	50	27	1.6×10^7	23
2	2	20	27	3.3×10^7	12

films, a second set of solar cells was prepared with a more elaborate process, which included bulk hydrogen passivation and a double layer ARC. For set 2, Table I summarizes the main film parameters. In addition to electrical solar cell characterization, these Si films were characterized by detailed dislocation density measurements. Emitter formation and metallization were identical for both sets of solar cells. The emitter was prepared by diffusion from a $POCl_3$ source targeting a sheet resistivity of 80 $\Omega/\square$. The emitter was contacted by a photolithographically defined grid on the front side with conventional structure, while the base was contacted by evaporating an aluminum frame in a trench around the active cell area. After metallization, the solar cells from set 2 were passivated at 350 °C for 30 min in a remote hydrogen plasma. Finally, on these devices, a double layer ARC was applied. A more detailed description of the device structure is given in Ref. 17.

For electrical characterization of the thin-film solar cells, dark and illuminated I-V curves were measured. On set 2 I-V curves were measured before and after hydrogen passivation. On set 2 also internal quantum efficiency (IQE) curves were recorded and used to extract effective diffusion lengths. This was done after ARC deposition since at this state the lower reflection yields higher accuracy.

For an analysis of the crystallographic defects, mechanically polished samples were prepared from the Si films and treated 15–20 s with a Secco etch.[18] Etch pit density (EPD) maps were acquired using an automated microscope and specially developed image analysis algorithms. Details on the setup of this system are published elsewhere.[19] An average dislocation density value was calculated from the 14 000 to 32 000 data points in each EPD map. The method of averaging was chosen from the viewpoint of effective diffusion length. Let us assume that the effective diffusion length extracted from a full area IQE measurement has the value $L_{\mathrm{eff,IQE}}$. The average dislocation density $\bar{\rho}_d$ is then defined as the value that, in a reference device with homogeneously distributed dislocations, would yield the same effective diffusion length value $L_{\mathrm{eff,IQE}}$. To a first approximation, $L_{\mathrm{eff,IQE}}$ is linear in the logarithm of ρ_d. Therefore, the averaging was performed on the logarithmic EPD values.

III. ANALYTICAL MODEL

A. Donolato's model for the effect of dislocations

The starting point of our analysis is the dislocated semiconductor as modeled by Donolato.[4] The model assumes an array of straight dislocation lines perpendicular to the surface. The dislocation is characterized by its radius and a line recombination velocity, also referred to as recombination strength γ_d. Dividing γ_d by the diffusion constant D, we define the dimensionless parameter normalized recombination strength by $\Gamma_d \equiv \gamma_d/D$. The analytical solution to the boundary value problem contains an integration that cannot be carried out analytically. However, Donolato has also derived a closed form approximation, which reads[4]

$$L_{\mathrm{eff}}(\rho_d) \cong \left\{ \frac{1}{L_0^2} + \frac{\rho_d \Gamma_d}{1+(\Gamma_d/2\pi)[-\ln(\varepsilon\sqrt{\pi\rho_d})-C+(1/2)]} \right\}^{-1/2}, \tag{1}$$

where L_0 is the minority carrier diffusion length in the semiconductor without dislocations, ρ_d is the dislocation density, ε is the radius of the dislocation core, and C is Euler's gamma constant, with numerical value ≈0.577 216.

B. Extension of the model

For our purpose, we have modified the model with respect to two features: (i) the use of the "quantum efficiency effective diffusion length," which is compatible with the common analysis of quantum efficiency data, and (ii) the modeling of devices with finite thickness and finite surface recombination velocity (SRV) at the rear side. In the following sections an outline of the modified model is given. More details, including numerical simulations that support the approximation involved in step (ii), are given elsewhere.[20]

1. Quantum efficiency effective diffusion length

Donolato analyzed the dislocated semiconductor based on the charge collection probability function $\varphi(\mathbf{r})$. He introduced a special definition of "effective diffusion length," which is proportional to the integral over $\varphi(\mathbf{r})$

$$L_{\mathrm{eff},D} = \frac{1}{A}\int_{V_c} \varphi(\mathbf{r})\,dV, \tag{2}$$

where A is the area of the junction at $z=0$ and V_c is the volume of the (unit) cell.

From practical and physical points of view, there are some disadvantages in this definition. Among others, $L_{\mathrm{eff},D}$ is not compatible with standard measurement methods that rely on the slope of the curve of inverse quantum efficiency

IQE^{-1} versus absorption length α^{-1}. Moreover, the operational state of homogeneous generation, on which the definition is based on, does not correspond to the typical operation conditions of a solar cell. Photons with near band-gap wavelength contribute to a very small part of total irradiated energy only.

Therefore, in our modeling we employed the *quantum efficiency effective diffusion length*.[21] This quantity is proportional to the spatial derivative of φ with respect to z, where the z direction is perpendicular to the p-n junction

$$\frac{1}{L_{\mathrm{eff,IQE}}} = \left.\frac{d\mathrm{IQE}^{-1}}{d\alpha^{-1}}\right|_{\alpha^{-1}=0} = \left.\frac{d\varphi(z)}{dz}\right|_{z=0}. \tag{3}$$

In the three-dimensional case, $\varphi(z)$ is the projection of $\varphi(\mathbf{r})$ on the z axis. It is computed by integrating φ over x and y (or r and θ in cylindrical coordinates) and division by A. The connection between the term in the middle and the one on the right hand side is due to the important identity of current voltage and quantum efficiency effective diffusion length (which holds as long as potential fluctuations are absent).[22] The relationships involved are the dependence of the saturation current density J_0 on $\varphi(z)$ (Ref. 10),

$$J_0 = qn_0D \left.\frac{d\varphi(z)}{dz}\right|_{z=0}, \tag{4}$$

where n_0 is the minority carrier equilibrium concentration and q is the elementary charge, and the definition of the *current voltage effective diffusion length*[23]

$$L_{\mathrm{eff},J_0} = \frac{qDn_0}{J_0}. \tag{5}$$

Using the above mentioned identity $L_{\mathrm{eff,IQE}}=L_{\mathrm{eff},J_0}$, insertion of Eq. (4) into Eq. (5) and inversion of the term yields the right hand side of Eq. (3). Referring to Eq. (4), we note that the treatment of the three-dimensional case can equally be accomplished by integrating J_0 over x and y (or r and θ) and dividing the resulting current by A, yielding an average J_0.

2. Thin devices with finite SRV

In the investigated thin-film solar cells, the typical bulk diffusion length is of the same magnitude as the thickness of the active Si film. Device modeling as a semi-infinite specimen is therefore not applicable. In Ref. 4 a solution for the problem of finite thickness and infinite SRV has been derived. However, in our devices, the p-p+ junction implements a so-called back surface field (BSF) with a finite effective surface recombination velocity. In this case, due to the boundary condition at the rear, the solution to the differential equation for $\varphi(\mathbf{r})$ cannot be separated into an axial and a radial part.[20] For that reason, we have developed an approximate solution, which involves two steps: (i) calculation of a bulk diffusion length $L_{\mathrm{eff},b}$ for the case of a dislocated semi-infinite specimen and (ii) treating the dislocated Si as homogeneous material with bulk diffusion length $L_{\mathrm{eff},b}$, which is "cut off" at a length W_1 by applying the appropriate boundary condition for the back surface. The main argument for this approach from a physical point of view is the finding

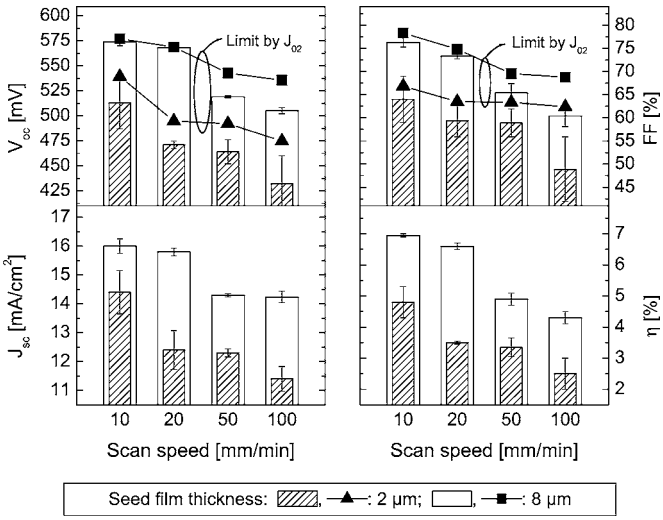

FIG. 1. Dependence of solar cell parameters on ZMR scan speed, for devices fabricated from epitaxially thickened 2 and 8 μm thick seed films, respectively. Bars represent measured data, while symbols show calculated values, which were derived from saturation current densities. Data are for solar cells without surface texturing, hydrogen passivation, and ARC.

that the typical effective diffusion length in the semiconductor $L_{\mathrm{eff},b}$ (the mean free path of the charge carriers) is larger than the average dislocation distance.

In practice, we performed step (i) by setting $L_{\mathrm{eff},b}=L_{\mathrm{eff}}(\rho_d)$, where $L_{\mathrm{eff}}(\rho_d)$ is the dependence as derived by Donolato for the semi-infinite specimen, either given by approximation (1) or by the exact form provided in Ref. 4. In the case of the semi-infinite geometry, the projection of $\varphi(\mathbf{r})$ on the radial axis, $\varphi(z)$, can very well be approximated by the one-dimensional exponential function $\exp(-z/L_{\mathrm{eff}})$.[20] Therefore, in this special case, the value of $L_{\mathrm{eff},b}$ is the same whether we use Donolato's definition of effective diffusion length [Eq. (2)] or the quantum efficiency effective diffusion length [Eq. (3)].

Step (ii) can be considered as taking a "slice" of thickness W_1 from the dislocated material with homogeneous diffusion length $L_{\mathrm{eff},b}$. The charge collection probability function $\varphi(z)$ is obtained as solution to the transport equation with boundary conditions $\varphi(0)=1$ and $d\varphi/dz=-s_1\varphi$ at $z=W_1$ which reads

$$\varphi(z) = \frac{\cosh[(W_1-z)/L_{\mathrm{eff},b}] + L_{\mathrm{eff},b}s_1 \sinh[(W_1-z)/L_{\mathrm{eff},b}]}{\cosh(W_1/L_{\mathrm{eff},b}) + L_{\mathrm{eff},b}s_1 \sinh(W_1/L_{\mathrm{eff},b})}, \tag{6}$$

where $s_1=S_1/D_1$ denotes the reduced back surface recombination velocity at the rear side, and D_1 is the minority carrier diffusion constant. The final term for $L_{\mathrm{eff,IQE}}$, which considers recombination at the dislocations as well as at the rear surface, is obtained by inserting Eq. (6) into Eq. (3).

IV. RESULTS AND DISCUSSION

Figure 1 shows illuminated solar cell parameters (bars) in dependence of ZMR scan speed, measured on solar cells from set 1. With increasing ZMR scan speed all I-V curve parameters decrease significantly. The behavior is similar for devices from 2 μm as well as from 8 μm thick seed films.

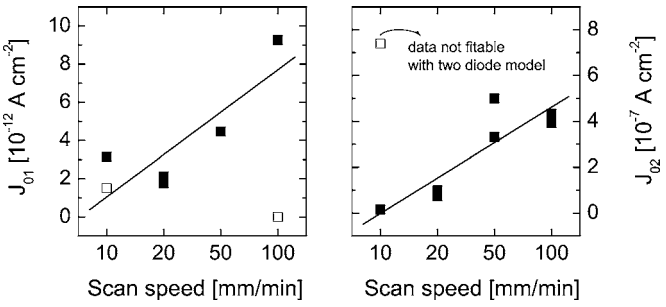

FIG. 2. Dependence of saturation current densities J_{01} and J_{02} on ZMR scan speed for devices from 8 μm thick see films. Data are for solar cells without surface texturing, hydrogen passivation, and ARC. It was measured on the same devices for which the illuminated parameters are shown in Fig. 1.

The decrease of the electrical parameters is in accordance with the observed increase in defect density, mainly in the form of dislocations. Additionally, dark *I-V* curves were measured on the same solar cells and fitted with the two-diode model,

$$J(V) = J_{01}\{e^{q[V-J(V)R_s]/n_1k_BT} - 1\} + J_{02}\{e^{q[V-J(V)R_s]/n_2k_BT} - 1\} + \frac{V-J(V)R_s}{R_p} - J_L, \quad (7)$$

where J_{01} is the current density due to recombination in emitter and base, J_{02} is the SCR recombination current density, and R_s and R_p are series and shunt resistances, respectively. k_B denotes the Boltzmann constant, T the absolute temperature, and q the elementary charge. Using $n_1=1$ and $n_2=2$, Eq. (7) could be well fitted to data from 8 μm seed film devices. On devices from the more defective 2 μm thick seed films, the curves deviated significantly from the ideal behavior and only the parameter J_{02} could be obtained reliably. The parameters J_{01} and J_{02} show a systematic increase with increasing ZMR scan speed (Fig. 2). Particularly high are the J_{02} values. To study the effect of J_{02} on open circuit voltage more quantitatively, V_{oc} and fill factor (FF) were computed by the two-diode model, taking the experimentally determined J_{02} values as input parameters. All other parameters were kept fixed using typical experimental data of a good solar cell: $J_L=15$ mA cm^{-2}, $J_{01}=3\times10^{-12}$ A cm^{-2}, $R_p=10\,000\ \Omega$, and $R_s=1.1\ \Omega$ (for 8 μm thick seed films) or $R_s=2.1\ \Omega$ (for 2 μm thick seed films). The calculated values are plotted additionally in Fig. 1 (symbols) resembling the trend of the experimental values. We conclude that the observed decrease in V_{oc} and FF is largely due to a high SCR recombination current density J_{02}.

Data of L_{eff} and V_{oc} versus dislocation density, measured on solar cells from set 2, are shown in Fig. 3. The three characterized samples (Table I) represent typical devices with significantly different dislocation densities. Dislocation density in the device with lowest effective diffusion length (2 μm thick seed film, 20 mm min^{-1} scan speed) is about four times as high as in the device with highest effective diffusion length (8 μm thick seed film, 20 mm min^{-1} scan speed). We also fabricated devices with even higher defect density. However, in this range optical counting of etch pits is not reliable anymore due to a huge portion of clustered etch pits. Additionally, dark *I-V* curves of these devices de-

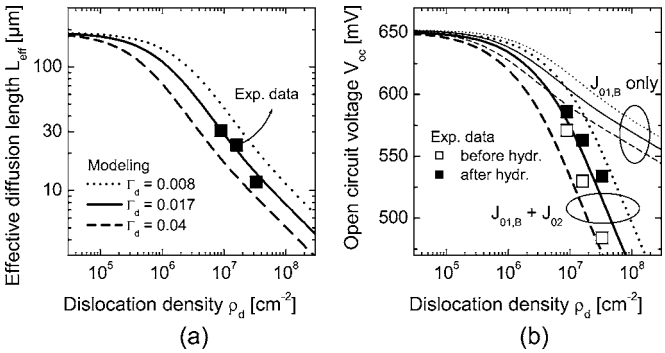

FIG. 3. (a) Dependence of effective diffusion length L_{eff} on dislocation density. The experimental data points $L_{eff,i}(\rho_{d,i})$ (given in Table I) are fitted with the modified version of Donolato's model. Modeled curves are shown for the recombination strength value yielding the best fit ($\Gamma_d=0.017$), as well as for $\Gamma_d=0.008$ and $\Gamma_d=0.04$. (b) Dependence of open circuit voltage V_{oc} on dislocation density. The relationship is modeled using the same recombination parameters as in part (a). The curves drawn with thin lines take into account a dislocation dependence on $J_{01,B}$ only, while those drawn with thick lines additionally consider SCR recombination (J_{02}). Fixed parameters were $\varepsilon=0.01$ μm, $W_1=27$ μm, and $s=0.004$ μm^{-1}. Except for the points drawn with open symbols, data are for devices with hydrogen passivation and double layer ARC.

viated significantly from the ideal behavior ($n_1=1$, $n_2=2$). Therefore, on these devices the proposed model is not applicable.

As can be taken from Table I, Si film thickness and effective diffusion length are in the same range, and therefore strictly speaking, the function IQE$^{-1}(\alpha^{-1})$ cannot be described by a linear relationship. Thus, for the solar cell with the highest diffusion length, we fitted the exact nonlinear curve resulting from the solution of the appropriate boundary value problem[24] to the measured quantum efficiency data. The effective recombination velocity S_1 at the low-high junction between p epitaxial layer and $p+$ seed layer was taken as 750 cm s^{-1}. This value was calculated from doping and thickness data using the expression given in Ref. 25 and taking into account band-gap narrowing. Then, based on the data from the fit by the exact function, the error made when using the approximate linear fit was quantified. The calculated systematic error is below 2% relative, and therefore it is negligible compared to the error stemming from measurement inaccuracies of the IQE data. In conclusion, the more sophisticated fitting routine does not yield improved accuracy in this case. For that reason, all effective diffusion length values in Table I were determined by linear fitting.

In our model, we did not account for a possible dislocation dependence of the effective surface recombination velocity S_1 at the p-$p+$ low-high junction. However, we performed a sensitivity analysis in order to estimate the possible error. For the device with $L_{eff}=30$ μm (Table I) a doubling of S_1 results in a decrease of L_{eff} by 1 μm. For devices with higher dislocation density, L_{eff} is smaller and therefore less sensitive on S_1. For $L_{eff}=12$ μm an increase of S_1 by a factor of 10 reduces L_{eff} just by about 0.1 μm.

In Fig. 3(a) the data of $L_{eff,IQE}$ vs. ρ_d from Table I are plotted together with simulated curves using the modified Donolato model [given through Eqs. (1), (6), and (3)]. Taking $\varepsilon=0.01$ μm, $W_1=27$ μm, and $s_1=S_1/D_1=0.004$ μm^{-1} as

fixed parameters, the best fit values obtained are $L_0 = 119\ \mu$m and $\Gamma_d = 0.017$. Additional curves are plotted for recombination strength values of approximately one-half and two times the best fit value (i.e., $\Gamma_d = 0.008$ and $\Gamma_d = 0.04$). Note that in logarithmic scale, a variation in Γ_d yields a parallel displacement of the L_{eff} vs. ρ_d curve.

Based on his model for the effect of dislocations on effective diffusion length, Donolato has also calculated the effect on open circuit voltage V_{oc}.[10] In this work he considered the dislocation dependence of V_{oc} through the base saturation current $J_{0,B}$. The open circuit voltage V_{oc} is then determined by

$$V_{\text{oc}} = \frac{k_B T}{q} \ln\left[\frac{J_L}{J_{0,B}(\rho_d)} + 1\right] = \frac{k_B T}{q} \ln\left[\frac{J_L L_{\text{eff}}(\rho_d)}{q D_n n_0} + 1\right]. \tag{8}$$

As light generated current J_L we inserted the maximum J_{sc} value ($=17.7\ \text{mA cm}^{-2}$) measured on the three solar cells listed in Table I.

In the investigated solar cells, V_{oc} is strongly affected by SCR recombination, as discussed before. In order to account for this effect, the forward bias recombination current J_{rg} was considered by means of the theory by Sah *et al.*[26] describing the forward bias SCR recombination current J_{rg}^+ through

$$J_{\text{rg}}^+(V) = \underbrace{\frac{q W_{\text{eff}} n_i}{2\tau_0}}_{J_{02}} \left[\exp\left(\frac{qV}{2k_B T}\right) - 1\right]. \tag{9}$$

In the above equation n_i is the intrinsic carrier concentration, τ_0 is the carrier lifetime in the SCR, and W_{eff} is the effective thickness of the recombination region. The recombination rate is highest at the location with maximum field strength and quickly decreases on either side of the maximum. Therefore, in the approximate expression by Sah *et al.* recombination is not considered in the complete SCR, but in a narrower region of width W_{eff} only. The SCR lifetime τ_0 was replaced by the function $L_{\text{eff}}(\rho_d)^2 / D_n$. For simplification, equal lifetimes were taken for both carrier types ($\tau_p = \tau_n$), mobilities for p-type quasineutral and SCR were assumed to be equal, and band-gap narrowing was neglected. The term for J_{02} from Eq. (9) was inserted into the two-diode model equation (7), which was solved for V_{oc} with $R_s = 0$, $R_p = \infty$, $n_1 = 1$, and $n_2 = 2$.

The resulting curves are plotted in Fig. 3(b) (thick lines). While a change in the recombination strength Γ_d produces a parallel shift of the curve, the slope is determined by the nature of the recombination channel. In the quasineutral region, the recombination current is proportional to $\tau^{-1/2}$ [Eq. (5), and $L = (D\tau)^{1/2}$], while in the SCR it is proportional to τ^{-1} [Eq. (9)]. Therefore, in the later case a much steeper decrease of the V_{oc} vs. ρ_d curve is found.

To fit the model to the experimental data, the effective width of the SCR W_{eff} was used as additional variable parameter, yielding an optimal result for $W_{\text{eff}} = 1\ \mu$m [thick lines in Fig. 3(b)]. This value is much larger than estimations for W_{eff} obtained from a numerical modeling of the investigated solar cell structure with the software PC1D.[27] In this simulation, a maximum field strength E_{max} of $\sim 33\ \text{kV cm}^{-1}$ was found. Inserting this value into the approximation given in Ref. 26 yields $W_{\text{eff}} = k_B T / \pi q E_{\text{max}} = 0.025\ \mu$m. A similar value for E_{max} is obtained using the linear potential variation $E_{\text{max}} = 2(V_{\text{bi}} - V)/W_{\text{scr}}$. The values $V_{\text{bi}} - V \approx V_{\text{bi}} = 0.6$ V (small forward bias) and $W_{\text{scr}} = 0.17\ \mu$m, estimated from PC1D simulations, lead the effective width $W_{\text{eff}} = 0.023\ \mu$m.

Instead of an increase of W_{eff}, the enlarged J_{02} component could equally be attributed to an increase of the intrinsic carrier concentration or a decrease in the lifetime τ_0 [see Eq. (9)]. It has to be kept in mind that Donolato's model is based on a solution of the transport equation in quasineutral regions and it does not consider electric fields. The consideration of such electric fields could be important if recombination at dislocations is not adequately described by the Shockley-Read-Hall model but with the model of charge-controlled recombination as proposed by Wilshaw and Fell.[28–30]

However, results on fine-grained Si films support the theory of a pure geometric enlargement of the SCR. For thin-film solar cells from fine-grained Si films, Beaucarne *et al.* found that the width W_{eff} has to be much wider than the effective width derived from the maximum field strength, in order to explain the measured recombination current. Firstly, they proposed an extension of the SCR due to depleted grains, caused by a high density of grain boundaries.[31] Later they modified their model and explained their experimental findings by preferential diffusion of phosphorus at grain boundaries.[32] The replacement of the diffused junction by a heterojunction indeed led to a strong decrease of the SCR saturation current and supports the latter interpretation.[33]

In analogy, in the Si thin films studied in this work, preferential diffusion of phosphorus at dislocations and/or grain boundaries may extend the junction area. For the devices investigated in Ref. 32, in addition an increase of carrier collection efficiency has been observed. In contrast, in our devices effective diffusion length decreases with increasing dislocation density (see Table I). However, this finding can be explained by the ratio of effective SCR width W_{eff} to effective diffusion length L_{eff}. The dimension of W_{eff} was found to be $\sim 1\ \mu$m, while for L_{eff} values were in the range of $12-30\ \mu$m. Therefore, the effect of enhanced carrier collection would be negligible. An additional effect of the preferential doping might be an effective decrease of the emitter doping concentration. This effect could decrease the electric field and therefore enhance the width W_{eff} as argued in Ref. 33.

V. CONCLUSIONS

Based on Donolato's model for the effect of dislocations on minority carrier effective diffusion length the dependence of open circuit voltage on dislocation density has been modeled. The experimental data were acquired on crystalline silicon thin-film solar cells. To account for finite cell thickness and finite recombination velocity at the rear side we used an extended version of Donolato's model developed before. Experimental data showed a strong decrease of open circuit voltage with increasing dislocation density. Dark I-V curve measurements indicate that the saturation current is dominated by recombination in the SCR. Our model fits well the

experimental data if both components, the base recombination current as well as the SCR recombination current, are taken into account. Usually the region of high recombination is restricted to an "effective width" being smaller than the SCR induced by the *p-n* junction. However, satisfactory fitting results require that this region is set wider than the "effective depletion region width," which is calculated from the electrical field strength in a planar *p-n* junction. This effect can be explained with the assumption of a geometrical enlargement of the *p-n* junction due to defects like dislocations.

ACKNOWLEDGMENTS

The authors would like to thank the technical staff from the Fraunhofer ISE Solar Cell Department for device processing and conducting measurements. They are grateful to Ch. Schmiga from ISFH Hameln/Emmerthal who carried out the hydrogen passivation. One of the authors (T.K.) has been supported by the scholarship program of the German Federal Environmental Foundation. They acknowledge support by the government of the state of Baden-Württemberg within the FAKT project.

[1]H. El Ghitani and S. Martinuzzi, J. Appl. Phys. **66**, 1723 (1989).
[2]M. Imaizumi, I. Tadashi, M. Yamaguchi, and K. Kaneko, J. Appl. Phys. **81**, 7635 (1997).
[3]T. Kieliba, J. Pohl, A. Eyer, and C. Schmiga, in *Proceedings of the Third World Conference on Photovoltaic Energy Conversion*, edited by K. Kurokawa, L. L. Kazmerski, B. McNelis, M. Yamaguchi, C. Wronski, and W. C. Sinke (WCPEC-3 Organizing Commitee, Osaka, 2003), Vol. B, pp. 1170–1173.
[4]C. Donolato, J. Appl. Phys. **84**, 2656 (1998).
[5]A. Lawerenz, M. Rinio, S. Riedel, M. Ghosh, M. Werner, and H. J. Möller, in *Proceedings of the 16th European Photovoltaic Solar Energy Conference, Glasgow, UK, 2000*, edited by H. Scheer, B. McNelis, W. Palz, H. A. Ossenbrink, E. Dunlop, and P. Helm (James & James Ltd., London, 2000), pp. 1647–1650.
[6]S. Riedel, M. Rinio, and H. J. Möller, in *Proceedings of the 17th European Photovoltaic Solar Energy Conference, Munich, 2001*, edited by W. Palz, B. McNelis, H. A. Ossenbrink, and P. Helm (WIP Renewable Energies, Munich, 2001), pp. 1412–1415.
[7]M. Rinio, S. Peters, M. Werner, A. Lawerenz, and H. J. Möller, *Proceedings of the Ninth International Autumn Meeting on Gettering and Defect Engineering in Semiconductor Technology (GADEST 2001) Catania, Italy, 2001* [Solid State Phenom. **82–84**, 701 (2002)].
[8]M. Rinio, A. Hauser, and H. J. Möller, in *Proceedings of the Third World Conference on Photovoltaic Energy Conversion, Osaka, 2003*, edited by L. L. Kazmerski, K. Kurokawa, B. McNelis, M. Yamaguchi, C. Wronski, and W. C. Sinke (WCPEC-3 Organizing Committee, Osaka, 2003), Vol. A, pp. 118–121.
[9]M. Rinio, E. Zippel, and D. Borchert, in *Proceedings of the 20th European Photovoltaic Solar Energy Conference and Exhibition, Barcelona, Spain, 2005*, edited by W. Palz, H. Ossenbrink, and P. Helm (WIP-Renewable Energies, Munich, 2005), pp. 706–709.
[10]C. Donolato, *Proceedings of the Fifth International Workshop on Beam Injection Assessment of Defects in Semiconductors (BIADS 98), Schloss Wulkow, Germany, 1998* [Solid State Phenom. **63–64**, 45 (1998)].
[11]M. J. Keevers and P. P. Altermatt, in *Proceedings of the 16th European Photovoltaic Solar Energy Conference*, edited by H. Scheer, B. McNelis, W. Palz, H. A. Ossenbrink, E. Dunlop, and P. Helm (James & James Ltd., London, 2000), Vol. II, pp. 1759–1762.
[12]J. M. Keevers, A. Turner, U. Schubert, P. A. Basore, and M. A. Green, in *Proceedings of the 20th European Photovoltaic Solar Energy Conference and Exhibition, Barcelona, Spain, 2005*, edited by W. Palz, H. Ossenbrink, and P. Helm (WIP-Renewable Energies, Munich, 2005), pp. 1305–1308.
[13]H. Naomoto, S. Hamamoto, A. Takami, S. Arimoto, and T. Ishihara, Sol. Energy Mater. Sol. Cells **48**, 261 (1997).
[14]A. Takami, S. Arimoto, H. Naomoto, S. Hamamoto, T. Ishihara, H. Kumabe, and T. Murotani, *Proceedings of the First World Conference on Photovoltaic Energy Conversion, Waikoloa, HI, 1994* (IEEE, New York, 1994), Vol. 2, pp. 1394–1397.
[15]S. M. Yoon and I. N. Miaoulis, *Proceedings of the Kinetics of Phase Transformations Symposium, Boston, MA, 1990*, edited by M. O. Thompson, M. J. Aziz, and G. B. Stephenson [Mater. Res. Soc. Symp. Proc. **205**, 453 (1992)].
[16]S. M. Yoon and I. N. Miaoulis, J. Appl. Phys. **72**, 316 (1992).
[17]S. Reber, W. Zimmermann, and T. Kieliba, Sol. Energy Mater. Sol. Cells **65**, 409 (2001).
[18]F. Secco D'Aragona, J. Electrochem. Soc. **119**, 948 (1972).
[19]T. Kieliba, Ph.D. thesis, Universität Konstanz, 2006.
[20]T. Kieliba, S. Riepe, and W. Warta, J. Appl. Phys. **100**, 063706 (2006).
[21]R. Brendel, *Thin-Film Crystalline Silicon Solar Cells: Physics and Technology* (Wiley-VCH, Weinheim, 2003), p. 55.
[22]R. Brendel and U. Rau, J. Appl. Phys. **85**, 3634 (1999).
[23]R. Brendel, *Thin-Film Crystalline Silicon Solar Cells: Physics and Technology* (Wiley-VCH, Weinheim, 2003), p. 56.
[24]J. Isenberg, O. Bartels, and W. Warta, *Proceedings of the 29th IEEE Photovoltaic Specialists Conference, New Orleans, LA, 2002* (IEEE, New York, 2002), pp. 328–331.
[25]M. P. Godlewski, C. R. Baraona, and H. W. Brandhorst, Sol. Cells **29**, 131 (1990).
[26]C. T. Sah, R. N. Noyce, and W. Shockley, Proc. IRE **45**, 1228 (1957).
[27]D. A. Clugston and P. A. Basore, *Proceedings of the 26th IEEE Photovoltaic Specialists Conference, Anaheim, CA, 1997* (IEEE, New York, 1997), pp. 207–210.
[28]P. R. Wilshaw and T. S. Fell, *Proceedings of the Sixth International Symposium on the Structure and Properties of Dislocations in Semiconductors*, edited by S. G. Roberts, D. B. Holt, and P. R. Wilshaw [Inst. Phys. Conf. Ser. **104**, 85 (1989)].
[29]T. S. Fell and P. R. Wilshaw, in *Sixth International Symposium on the Structure and Properties of Dislocations in Semiconductors*, edited by S. G. Roberts, D. B. Holt, and P. R. Wilshaw (Institute of Physics, Bristol, 1989), pp. 227–232.
[30]M. Kittler and W. Seifert, *Fourth International Workshop on Beam Injection Assessment of Defects in Semiconductors (BIADS 96), Escorial, Spain* [Mater. Sci. Eng., B **42**, 8 (1996)].
[31]G. Beaucarne, J. Poortmans, M. Caymax, J. Nijs, and R. Mertens, IEEE Trans. Electron Devices **47**, 1118 (2000).
[32]G. Beaucarne, M. Caymax, I. Peytier, and J. Poortmans, Solid State Phenom. **80–81**, 269 (2001).
[33]L. Carnel, I. Gordon, D. Van Gestel, K. Van Nieuwenhuysen, G. Agostinelli, G. Beaucarne, and J. Poortmans, Thin Solid Films **511–512**, 21 (2006).